CRITICAL BEHAVIOR OF A $La_{0.7}Sr_{0.3}MnO_3$ CRYSTAL IN THE VICINITY OF ITS TRANSITION TO FERROMAGNETIC STATE

V.M. KALITA, A.F. LOZENKO, S.M. RYABCHENKO, P.O. TROTSENKO, A.I. TOVSTOLYTKIN[1], A.M. POGORILY[1]

Institute of Physics, Nat. Acad. of Sci. of Ukraine
(46, Nauky Ave., Kyiv 03680, Ukraine),

[1]**Institute of Magnetism, Nat. Acad. of Sci. of Ukraine and Ministry of Education and Science of Ukraine**
(36b, Academician Vernadsky Blvd., Kyiv 03680, Ukraine)

UDC 537.6

Magnetostatic properties of a $La_{0.7}Sr_{0.3}MnO_3$ single crystal have been studied in the vicinity of its critical temperature T_c. A nonlinear temperature dependence of the inverse magnetic susceptibility which is characteristic of the Griffiths phase, has been found in the minimal measuring magnetic field at temperatures slightly above the temperature of ferromagnetic (FM) ordering. A conclusion was made that such a nonlinearity arises owing to the formation of magnetic polarons. The applicability of the Belov–Arrott plots to the systems with the Griffiths phase has been analyzed, and their characteristic features have been revealed. These features have been demonstrated to present in the Belov–Arrott plots for the experimental data on $La_{0.7}Sr_{0.3}MnO_3$. It has been shown that the critical properties of the $La_{0.7}Sr_{0.3}MnO_3$ crystal are described by somewhat different sets of critical indices in the FM, $T < T_c$, and paramagnetic, $T > T_c$, phases.

1. Introduction

Researches of substituted manganites $La_{1-x}A_xMnO_3$, where A is a divalent ion, have drawn attention for a good many years. An application-oriented interest is associated here with a characteristic temperature-driven phase transition of the "paramagnetic insulator–FM metal" type and the presence of the colossal magnetoresistance (CMR) effect in its vicinity. Of no less interest is the problem to describe the properties of systems with randomly distributed variable valence, which include substituted manganites. Substitution of a part of La^{3+} ions by ions of divalent metals (Ca^{2+}, Sr^{2+}) invokes the necessity to compensate the excess charge. There emerges either a definite number of "holes" in the valence band of the crystal (which gives rise to the metal conductance, if the holes are mobile enough) or the random alternation of Mn^{3+} and Mn^{4+} ions (which results in a state with low conductance, if the holes are localized). Taking into account the exchange interaction between charge carriers and ions in the framework of the "double exchange" model [1] for holes with a finite hopping probability allows one to understand, at a qualitative level, a transition in these systems into an FM state together with a transition into a metal state.

In unsubstituted $LaMnO_3$, the interaction between Mn^{3+} ions is antiferromagnetic. At $T_N = 140$ K, this substance undergoes a paramagnet– antiferromagnet transition.

The ground state of Mn^{3+} in a cubic crystalline field is degenerate with respect to the orbital quantum number. It is characterized by the Jahn–Teller reduction of a symmetry in the nearest environment. As a consequence, in the substituted crystal, there appear ordered or randomly distributed deformations. Deformations also arise due to a difference between the ionic radii of La^{3+} and A^{2+}. Therefore, the sequence of phase transitions in manganites with different compositions depends on the type and the concentration of ions that replace La^{3+}. In some manganites – e.g., in $La_{0.7}Ca_{0.3}MnO_3$ – the transition into the FM state is of the first order, while in others – e.g., in $La_{0.7}Sr_{0.3}MnO_3$ – of the second one. The difference between the critical behaviors of manganites with a number of compositions in the vicinity of their phase transitions was studied in works [2, 3]. The results obtained were analyzed on the basis of the Banerjee criterion [4, 5] for magnetization isotherms in the Belov–Arrott[1] (BA) plot coordinates [6, 7], namely, M^2 versus H_i/M, where H_i is the internal magnetic field in the specimen, and M the corresponding specimen magnetization.

[1]Rather often, K.P Belov's works [6] are not referred to in the European and American scientific literature, and those plots are named "Arrott plots". It is not correct, as can be seen from the publication dates of Belov's [6] and Arrott's [7] works.

Non-uniform deformations in a magnetic system can induce a non-uniform local distribution of the FM transition temperature, T_c. Compounds with non-uniform T_c, which is distributed continuously within a certain temperature interval, reveal specific magnetic properties. They were coined as "Griffiths phases" [8,9]. The singularity in the Griffiths phase susceptibility takes place at the temperature T_c^* that is located within the T_c-distribution interval and perceived as a phase transition point for the entire specimen.

There is also another reason why manganites are inhomogeneous in the temperature interval that precedes the FM ordering. The transition from a localized state of charge carriers in manganites to a delocalized one, which is responsible for the insulator–metal transition related to the FM ordering, occurs within a certain temperature interval. Therefore, holes which acquire mobility can induce, even in the paramagnetic state, a local spin alignment of Mn ions in a confined volume, thus reducing the spin energy of the system. Simultaneously, holes become localized in a created potential well, which gives rise to the formation of "magnetic polarons" [10,11]. When approaching the phase transition point, the number and the dimension of magnetopolaronic "droplets", as well as the number of charge carriers in every of them, increase. At the phase transition, the "droplets" merge together and form the long-range FM order. The magnetic state of a crystal in the critical region, but a little above T_c, includes two phases in equilibrium (an "intermediate" state). The relative volumes of the para- and "droplet-like FM" (magnetopolaronic) phases depend on the temperature. The temperatures of magnetic polaron formation are different, so that, in this sense, the system should manifest the critical properties that would be similar to those of the Griffiths phase. The critical properties of manganites with the Griffiths phase were studied in works [12,13].

As was mentioned above, $La_{0.7}Sr_{0.3}MnO_3$ has a phase transition of the second order into the FM state, which was proved in a number of works (see, e.g., work [2]). Its transition temperature into the FM state (according to various sources, $T_c \approx 352 \div 370$ K) is the highest among those for substituted manganites. At the same time, the CMR manifestation is relatively moderate, being maximal near T_c.

The manifestation of magnetopolaronic effects in $La_{0.7}Sr_{0.3}MnO_3$ and other manganites was discussed in a number of works. Its critical behavior in the vicinity of the phase transition was analyzed on the basis of BA plots. Those plots can be substantiated in the framework of the Landau model of phase transitions of the second order. In this model, the critical index β is equal to $\frac{1}{2}$. An account of the differences between a real phase transition of the second order and that in the Landau model consists in introducing the critical indices β, γ, and δ as fitting parameters and "modifying" the BA plots. Namely, the dependences $m^{1/\beta}$ versus $(H_i/m)^{1/\gamma}$ are plotted [14]. At optimally selected β and γ, the isotherms for temperatures both above and below T_c are straight lines. The T_c-isotherm passes through the coordinate origin.

The Griffiths phase is not described by the model of phase transitions of the second order. Therefore, its BA isotherms cannot be straightened at any set of critical indices. Moreover, the T_c^*-isotherm should not pass through the coordinate origin. We are not aware of any attempts to analyze the applicability of BA plots to the Griffiths phase or any suggestions of their modifications for this purpose. Nevertheless, some authors (see, e.g., works [2,3,15]) draw such plots even if the attributes of the Griffiths phase manifest themselves substantially, without focusing attention on possible features of the plotting procedure in this case. In work [2], for instance, the BA plots for $La_{2/3}Sr_{1/3}MnO_3$ were drawn for data measured at fields $H < 10$ kOe. As a result, it was found that $T_c = 370$ K. At the same time, the BA plots for $La_{2/3}Sr_{1/3}MnO_3$ contained substantial deviations from straightened isotherms in their low-field sections (see Fig. 3 in work [2]), but the authors did not discuss them.

The critical behavior of $La_{0.7}Sr_{0.3}MnO_3$ was analyzed in work [15] on the basis of modified BA plots. The fields $H < 100$ kOe were used for measurements. The plots presented in that work did not contain isotherm deviations from straight lines in selected coordinates. It was found from the plots that $T_c = 354$ K. The discrepancy between T_c-data and isotherm shapes in works [2] and [15] can be due to different qualities of the specimens used, or it can be a consequence of different experimental and calculation techniques. In work [15], as well as in work [12], the conclusion was made that the presence of paraphase magnetization inhomogeneity in $La_{0.7}Sr_{0.3}MnO_3$ reveals itself only in some deviations of the critical indices β, γ, and δ from the values predicted by those models, where this inhomogeneities are not taken into consideration.

In this work, the magnetostatic measurements of characteristics of a $La_{0.7}Sr_{0.3}MnO_3$ single crystal have been carried out at temperatures close to the critical one. It was done to reveal the manifestations of the magnetic state inhomogeneity (Griffiths phase effects) in critical properties. We have also analyzed the characteristic

features of Griffiths phase manifestations in the Belov–Arrott plots.

2. Specimen Description and Measurement Technique

A cylindrical $La_{0.7}Sr_{0.3}MnO_3$ single crystal 7 mm in height and 4 mm in diameter, grown up by A.M. Balbashev at the Moscow Power Engineering Institute (MPEI), Russia, was studied. According to the specimen characterization carried out at the MPEI, the axis of the cylinder coincided with the [111] axis of cubic crystal lattices of $La_{0.7}Sr_{0.3}MnO_3$, and the specimen density was $\rho = 6.268$ g/cm^3. Magnetostatic fields make the axis of a specimen with the indicated shape to be a direction of easy magnetization. The cylinder was not an ellipsoid of revolution; therefore, the demagnetization field was not quite uniform in its definite part. It had to bring about the magnetization non-linearity at the transition from the multidomain into the homogeneous state. However, this effect was not taken into account, when the results were analyzed. The specimen was simulated as a uniaxial ellipsoid of revolution with the demagnetization factors N_{zz} and $N_{xx} = N_{yy}$, where the z-axis is directed along the cylinder axis, and the x- and y-ones are perpendicular to it. The magnitudes of N_{zz}, N_{xx}, and N_{yy} were determined from the field dependences of the magnetization, as is described below.

The magnetization was measured on a LDJ–9500 vibromagnetometer at the field $H \leq 10$ kOe. The temperature was stabilized by a standard system of this device. The absolute accuracy of the temperature measurement was ± 1 K, and the accuracy of the temperature stabilization in the course of magnetization curve measurements was ± 0.2 K.

3. Magnetization Data

The magnetization of the specimen was measured at 295 K $< T <$ 380 K, with the external field H being directed either along the cylinder axis ($H_\parallel$) or perpendicularly to it ($H_\perp$). The specimen was found to be paramagnetic at T above $352 \div 355$ K and FM below this temperature. No magnetization hysteresis (to within the measurement accuracy of ± 1 Oe) was observed in the FM state in the whole temperature range of measurements. In Fig. 1, the dependences $m(H_\perp)$ of the magnetic moment of the specimen per its mass unit on the field $H_\perp$ at various temperatures T are depicted. Characteristic of those dependences are their initial

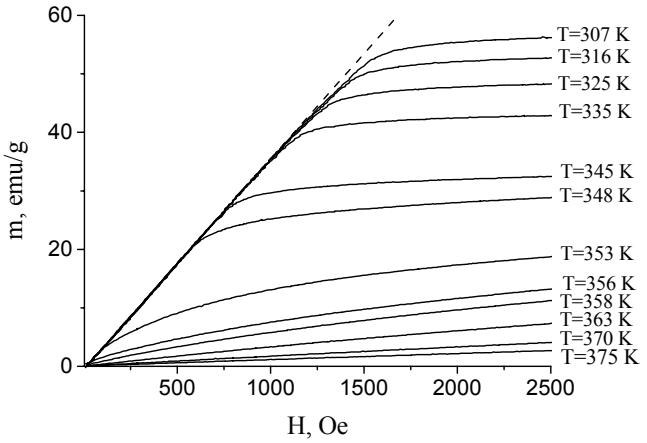

Fig. 1. Field dependences of the specimen magnetization on imposing a magnetic field perpendicularly to the specimen axis

linear sections, where the plot slope does not depend on T. The appearance of such sections is caused by the anisotropy effect generated by demagnetizing fields. In the fields that invoke rearrangements in the multidomain state, the magnetic moment per mass unit of the specimen, averaged over the specimen's volume, should be described at both orientations of the magnetic field ($H_\perp$ and $H_\parallel$) by the expression

$$\bar{m}_{\perp,\parallel} = H_{\perp,\parallel}/(\rho N_{\perp,\parallel}), \tag{1}$$

where $N_{\perp,\parallel}$ are the components of the demagnetization tensor for a specimen having the shape of a uniaxial ellipsoid of revolution, in a plane perpendicular to its axis and in the direction parallel to the latter, respectively. The magnetization curves in the $H_\parallel$-case are similar to those given in Fig. 1, but the slopes of the initial linear sections are lower, because $N_\parallel < N_\perp$ for our specimen. The slopes of those sections at different H-directions allowed the values $N_\parallel = N_{zz} = 2.9 \pm 0.1$ and $N_\perp = N_{xx} = N_{yy} = 4.5 \pm 0.1$ to be found. The sum $N_\parallel + 2N_\perp = 11.9 \pm 0.3 \approx 4\pi$. These values agree with estimations of work [16] made for the tensor components of demagnetization factors in the case of an ellipsoid, for which the ratio between its axis lengths is close to that between the height and the diameter of the specimen.

The absence of a hysteresis in the specimen magnetization was a certain surprise for us. At the initial stage, the magnetization occurs through the motion of domain boundaries. Owing to a low anisotropy of the specimen under investigation, the domain walls in it may be reasonably considered wider than the characteristic dimensions of structural defects, the latter playing the role of pinning centers. As a result, there are no barriers

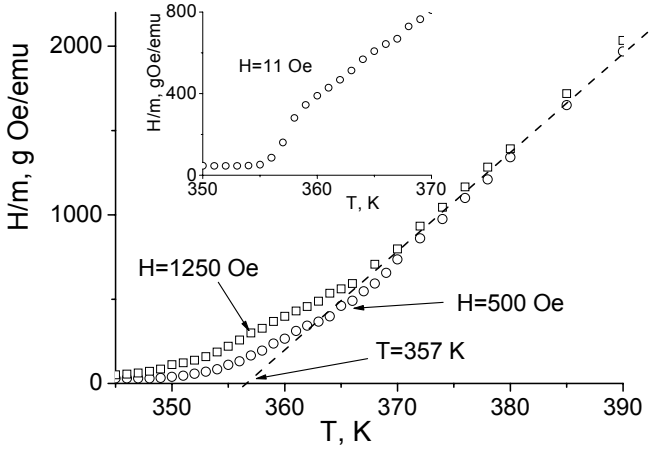

Fig. 2. Temperature dependences of H/m for $H = 500$ and 1250 Oe. The same dependence for $H = 11$ Oe is shown in the inset

for the walls to move freely, and that is why the hysteresis is absent. Certainly, it is possible only if the number of extensive defects is not appreciable; otherwise, they would impede even the motion of wide domain walls (pinning).

In a field that exceeds the demagnetizing threshold, the specimen is in a single-domain state, and the magnetization reaches a saturation, taking the paraprocess into account. The transition into the single-domain state is a little bit "smeared", which is testified by the deviations of the magnetization curves from dotted straight lines in Fig. 1. Besides the demagnetizing field nonuniformity, the transition into the "saturated" state can be made "smeared" by crystallographic anisotropy. To check this hypothesis, we measured the angular dependence of the specimen magnetization (along the applied field) in the fields $H_\perp$ that were both weaker and stronger than the saturation one. The specimen was rotated around its cylindrical axis, and the field was directed normally to it. Within the measurement accuracy, we did not find any manifestations of a magnetocrystalline anisotropy in the magnetization of the specimen.

A characteristic indicator of non-uniform regions that are ordered at temperatures higher than the FM ordering temperature in the whole specimen is the non-linearity of the temperature dependence of the inverse magnetic susceptibility $\chi^{-1}(H = \text{const}, T)$ at temperatures slightly higher than T_c^*. As a rule, this non-linearity is well pronounced at $H \to 0$, but it disappears at strong fields. In Fig. 2, the dependences $\chi^{-1}(H = \text{const}, T)$ are shown for $H = 11$, 500, and 1250 Oe. At $H = 11$ Oe, the non-linearity concerned (a "hockey stick") is evident.

The influence of demagnetizing fields, $\rho N_{\parallel,\perp} m(H,T)$, is reflected in the dependences $m(H = \text{const}, T)_{\text{ZFC}}$ registered in the course of the specimen heating after its cooling from $T > T_c$ at $H = 0$ [zero field cooling (ZFC)]. If the field H is strong enough to overcome the polydomain structure at all temperatures, the dependence $m(H = \text{const}, T)_{\text{ZFC}}$ falls down, when the specimen is heated up. At low fields ($H \to 0$), the dependence $m(H = \text{const}, T)_{\text{ZFC}}$ first grows as $/\,T$ increases, reaches its maximum in the vicinity of T_c, and then falls down. The emergence of a maximum in $m(H = \text{const}, T)_{\text{ZFC}}$ at low fields can be easily explained, if one considers the magnetic susceptibility in the internal field $H_i = H - \rho N_\perp m(H,T)$. In the case of the magnetization in the field $H_\perp$, the corresponding expression is

$$\chi(H_i, T) = \frac{m(H_\perp, T)}{H_\perp - N_\perp \rho m(H_\perp, T)}. \qquad (2)$$

Such dependences were measured in various $H_\perp$-fields. The maximum of $m(H = 11\ \text{Oe}, T)_{\text{ZFC}}$ was observed at $T = 353$ K, and it coincided with the maximum of $\chi(H_i,T)$. At the same time, the dependences $\frac{\partial}{\partial T} m(H = \text{const}, T)_{\text{FC}}$ revealed minima in the vicinity of T_c that corresponded to the inflection points in the $m(H = \text{const}, T)_{\text{FC}}$-curves. At $H = 11$ Oe, the minimum was observed at $T \approx 356$ K.

Now, to find T_c (or T_c^*) more accurately and to reveal whether the specimen contained FM inclusions, which became ordered before the FM order was established over the whole specimen, let us construct the corresponding BA plots.

4. Belov–Arrott Plots for the Griffiths Phase

First, let us discuss how the presence of the "Griffiths phase" in the specimen can reveal itself in BA plots. For this purpose, we carried out a computer simulation of the temperature dependence of the magnetization in various fields H and used the results obtained to calculate $\chi(H,T)$ and BA isotherms. We supposed that the specimen consisted of several parts. All parts were characterized by an identical magnetization of saturation, but every i-th part had its own temperature of FM ordering T_{ci}, different from the others, and all

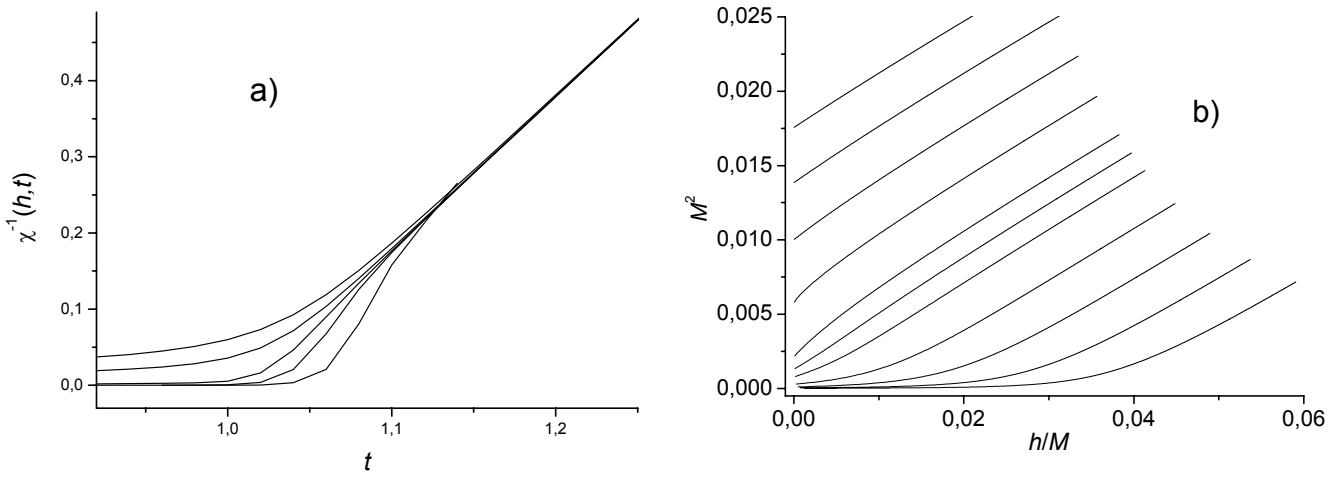

Fig. 3. Model dependences for a system with the Griffiths phase and an asymmetric exponential distribution function for relative volumes of the specimen with different local temperatures of magnetic ordering. Parameter $\Delta_{t_c} = \Delta_{T_c}/T_{c0} = 0.01$. (*a*) Theoretical dependences $\chi^{-1}(h,t)$. Curves from top to bottom correspond to the reduced magnetic field $h = 1\times10^{-2}$, 5×10^{-3}, 5×10^{-4}, 5×10^{-5}, and 5×10^{-6}, respectively. (*b*) Belov–Arrott isotherms. Curves from top to bottom correspond to the reduced temperatures $t = 0.985$, 0.99, 0.995, 1.0, 1.005, 1.0075, 1.01, 1.015, 1.02, 1.025, and 1.03, respectively

T_{ci} were distributed continuously around a definite T_{c0}. The relative (i.e. normalized by the saturation value) magnetization M_{ni} of the i-th part of the specimen was determined by seeking the solution of the equation obtained in the mean-field approximation (MFA) at a given external field H:

$$M_{ni} = B_s(x_{\rm MFA}), \tag{3}$$

where $B_s(x)$ is the Brillouin function for the spin S, $x_{\rm MFA} = S(g\mu_{\rm B}H + 3M_{ni}kT_{ci}/(S+1))/kT$, $\mu_{\rm B}$ is the Bohr magneton, and k the Boltzmann constant. We used the dimensionless temperature $t = T/T_{c0}$ and the dimensionless magnetic field $h = g\mu_{\rm B}HS/kT_{c0}$. Qualitative results do not depend on the selected spin magnitude. Therefore, for simplification, we used $S = 1/2$.

The relative volume of the specimen, in which the ordering temperature was T_{ci}, was described by the normalized distribution function $P_i(T_{ci}, T_{c0}, \Delta_{T_c})$, where Δ_{T_c} is the distribution parameter. The total normalized value for the specimen magnetization M was found by integrating the product $M_{ni}P_i(T_{ci}, T_{c0}, \Delta_{T_c})$ over the whole interval of possible T_{ci} values. We tried various distribution functions, both symmetric and asymmetric. For instance, the distributions $P_i(T_{ci}, T_{c0}, \Delta_{T_c}) = 0$ at $T_{ci} < T_{c0}$ and $P_i(T_{ci}, T_{c0}, \Delta_{T_c}) = \Delta_{T_c}^{-1}\exp[(T_{c0} - T_{ci})/\Delta_{T_c}]$ at $T_{ci} > T_{c0}$ (distribution I) or $P_i(T_{ci}, T_{c0}, \Delta_{T_c}) = 0$ at $T_{ci} < T_{c0}$ and $P_i(T_{ci}, T_{c0}, \Delta_{T_c}) = 2/(\Delta_{T_c}\sqrt{\pi})_{ci}^{-1}\exp[-(T_{c0}-T_{ci})^2/\Delta_{T_c}^2]$ at $T_{ci} > T_{c0}$ (distribution II) were analyzed. It is asymmetric distributions that simulate, in our opinion, the Griffiths phase with magnetopolaronic formations at temperatures higher than the temperature, at which the long-range order becomes established over the whole volume of the crystal.

In Fig. 3, the plots of the $\chi^{-1}(h = {\rm const}, t)$-dependence calculated in such a way for several h-values (panel *a*) and the BA plots in the vicinity of $t = t_{c0} = 1$ (panel *b*) are exhibited. The plots correspond to distribution I with $\Delta_{T_c} = 0.01T_{c0}$. It is evident that the plot in Fig. 3,*a* is qualitatively similar to that of the $\chi^{-1}(H = {\rm const}, T)$-dependence shown in Fig. 2. A characteristic "hockey stick" feature can be observed in $\chi^{-1}(t, h)$ with $h \to 0$, but it is smoothed for larger fields h.

The BA plots calculated for a system with no Griffiths phase, i.e. at $\Delta_{T_c} = 0$, are a collection of parallel straight lines, in which the isotherm for $T_c = T_{c0}$ passes through the coordinate origin. Figure 3,*b* demonstrates that if a finite Δ_{T_c} is taken into account, the initial sections of isotherms become curved; afterwards, they become linear. If the temperature changes from $T > T^*$ to $T < T^*$, where T^* is a certain temperature within the interval of the T_{ci}-distribution, the sign of the second derivative also changes in the initial sections of the curves. None of the isotherms passes through the coordinate origin. One of the isotherms, although not passing precisely through

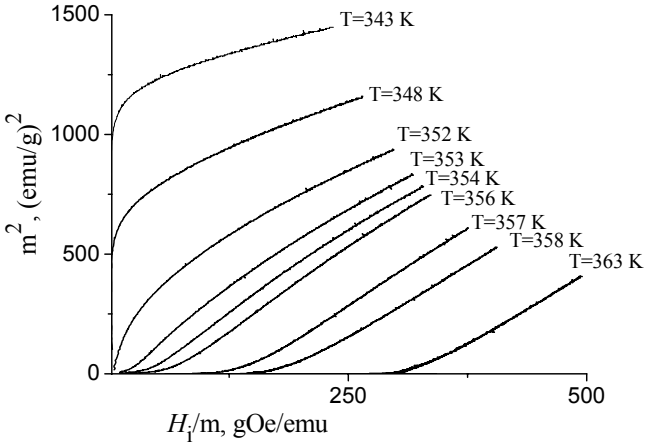

Fig. 4. Experimental dependences m^2 versus H_i/m (Belov–Arrott plots) for $La_{0.7}Sr_{0.3}MnO_3$ measured at various temperatures

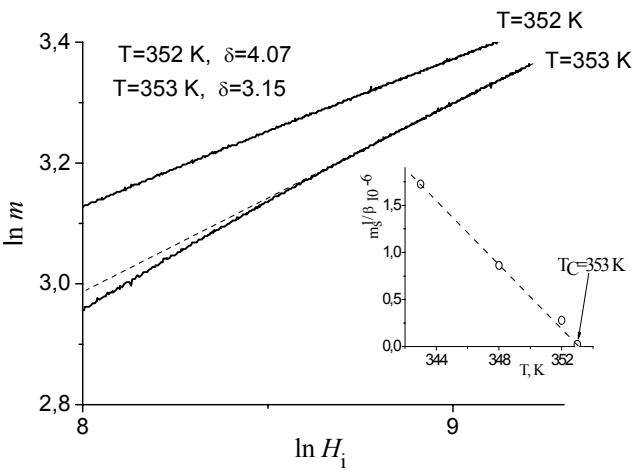

Fig. 5. Dependence $\ln m(H_i)$ on $\ln H_i$ for temperatures $T = 352$ and 353 K

the coordinate origin, is not bent in its initial section. Its corresponding temperature should evidently be referred to as $t_c^* = T_c^*/T_{c0}$.

Below, we will demonstrate that such features are observed in the BA plots drawn according to the results of our measurements of $m(H, T = \text{const})$ for $La_{0.7}Sr_{0.3}MnO_3$. They can also be seen in the BA plots of work [2], where the measurements were also carried out in fields $H \leq 10$ kOe. At the same time, they do not follow from the results of work [15], where the data for stronger fields were used, whereas the results of measurements in lower fields might probably be omitted.

5. Belov–Arrott Plots for $La_{0.7}Sr_{0.3}MnO_3$

To draw the BA plots [6, 7], we use the dependences $m(H, T = \text{const})$ obtained when the magnetic field $H_\perp$ was switched on. The corresponding correction of those dependences to demagnetizing fields will also be done.

In Fig. 4, the isotherms $m^2(H_\perp, T = \text{const})$ as the functions of H_i/m are shown for the studied $La_{0.7}Sr_{0.3}MnO_3$ specimen in the critical temperature range. Evidently, they are not parallel straight lines in the m^2 versus H_i/m coordinates. One can also see that, similarly to the model plots in the Griffiths phase case (Fig. 3,*b*), the temperature variation brings about the change of the second derivative sign. The curvature changes its sign in the temperature interval 353 K $< T <$ 355 K. The curvatures of curves in their initial sections testify that, although the manifestations of the Griffiths phase in $La_{0.7}Sr_{0.3}MnO_3$ are small, they appear not only in the $\chi^{-1}(T, H \to 0)$-dependences, but also in the BA plots. At the same time, the non-linearity of initial plot sections at temperatures T both above and below 353–356 K testifies that the critical indices for the given specimen do not correspond to the MFA model, i.e. $\beta \neq 1/2$.

According to Fig. 4, the curves for $T = 352$ and 353 K pass rather close to the coordinate origin. However, the initial section of the $T = 352$ K isotherm is curved in the same manner as all isotherms for $T > T^*$. The asymptote of its high-field section passes far enough from the coordinate origin. At the same time, the $T =$ 353 K isotherm separates curves with different signs of curvature of their initial sections, and the asymptote of its high-field section passes through the coordinate origin. As was indicated in Section 3, the temperature dependence $\chi(T, H \to 0)$ also has a maximum at $T =$ 353 K. Therefore, it is reasonable to suppose that this temperature corresponds to the effective temperature T_c^* of the specimen transition into the FM state.

In order to determine T_c^* in a more convincing way and to obtain the information on critical indices, it is necessary to modify the BA plots. Following work [14], we assume that the equation

$$(H_i/m)^{1/\gamma} = (T - T_c)T_1^{-1} + (m/m_1)^{1/\beta}, \tag{4}$$

where T_1 and m_1 are constant parameters, and β and γ are critical indices, holds true in the critical range. Then, the relation

$$(H_i/H_1) = (m/m_1)^\delta, \tag{5}$$

where H_1 is a constant, and $\delta = 1 + \gamma/\beta$, has to be obeyed at $T = T_c$. The index δ can be found from the dependence of $\ln m$ on $\ln H_i$ for $T = T_c$. These dependences are shown in Fig. 5 for $T = 352$ and 353 K.

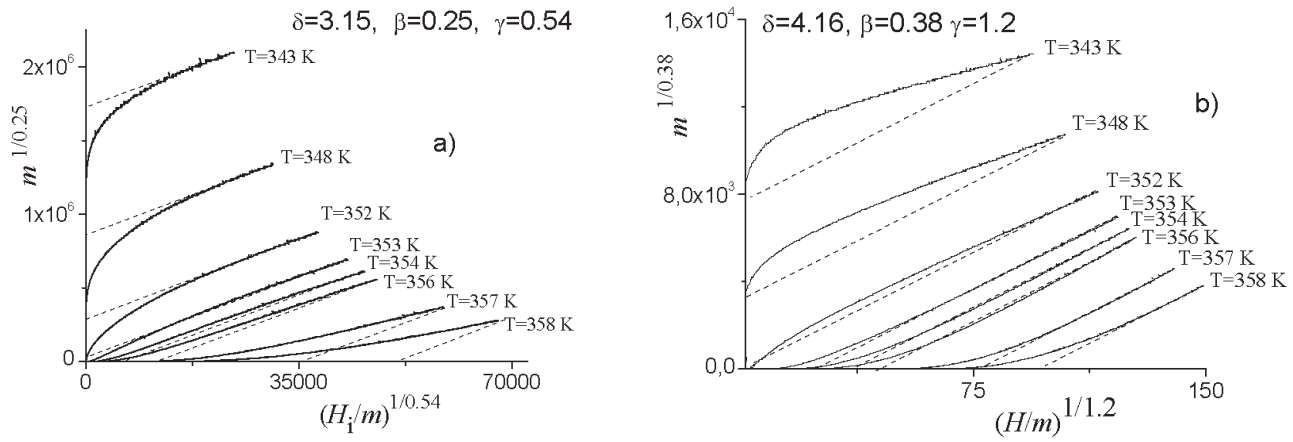

Fig. 6. Modified Belov–Arrott plots $m^{1/\beta}$ versus $(H_i/m)^{1/\gamma}$ for the $La_{0.7}Sr_{0.3}MnO_3$. (*a*) $\beta = 0.25$, $\gamma = 0.54$, and $\delta = 3.15$ ($T_c^* = 353$ K); (*b*) $\beta = 0.38$, $\gamma = 1.2$, and $\delta = 4.16$ ($T_c^* = 352$ K)

Calculating the slopes of their high-field sections (their asymptotes are plotted in Fig. 5 as dotted straight lines), we determined that $\delta = 3.15$ for $T = 353$ K, and $\delta = 4.16$ for $T = 352$ K.

Now, we must build the dependences $m^{1/\beta}$ versus $(H_i/m)^{1/\gamma}$ and find such β- and γ-values that satisfy the condition $\delta = 1 + \gamma/\beta$ and straighten those dependences. Taking the features of BA plots for systems with the Griffiths phase into account, we should try to straighten the high-field sections of isotherms. The best straightening of the curves for $T_c = 353$ K (i.e. at $\delta = 3.15$) was obtained at $\beta = 0.25$ and $\gamma = 0.54$ (see Fig. 6,*a*). To estimate the results of straightening and the parallelism of the curves visually, we drew some dotted lines parallel to the $T = T_c$ one in Figs. 6,*a* and *b*. One can see that the straightening and the parallelism of high-field sections of the curves take place for the FM states at $T < T_c$. At the same time, the curves for $T > T_c$ cannot be straightened at the selected values of critical indices even in their high-field sections. Two reasons can be responsible for that. First, the measurements were carried out at $T > T_c$ in the fields insufficiently strong to obtain linear high-field sections, free of the bending associated with the Griffiths phase. Second, the curves are not described at $T > T_c$ by the collection of indices determined for the FM phase.

Figure 6,*b* illustrates a modified BA plot for $\beta = 0.38$ and $\gamma = 1.2$. In this case, the curves at $\delta = 4.16$ (i.e. at $T_c = 352$ K) are better linearized, and the straightening and the parallelism of the curves are observed at $T > T_c$. However, for such values of β and γ, none of the curves for FM phase ($T < T_c$) can be straightened down to the coordinate origin, so that the curvature of the plots is too large.

Hence, for the studied $La_{0.7}Sr_{0.3}MnO_3$ specimen, the point of transition into the FM state corresponds to $T_c^* = 353$ K. At the same time, the critical indices for the FM and paramagnetic phases are somewhat different. As was discussed earlier, there appears an intermediate state at $T > T_c$ in the studied crystal, which is a paramagnetic phase with "magnetopolaronic FM droplets"; i.e. an analog of the Griffiths phase is realized. Different critical indices on each side of T_c does not follow from the BA plot analysis of the systems with the Griffiths phase, which was carried out in Section 4. The difference between the values of critical indices at $T < T_c$ and $T > T_c$ may arise due to a variation of the averaged amplitude of the exchange interaction in the specimen, which is connected with a change of its electric conductivity at a transition from the para- into the ferrophase.

Despite the discrepancy between the critical indices at $T < T_c$ and $T > T_c$, we should consider, bearing in mind our concept of the Griffiths phase, that the phase transition into the FM state occurs continuously, i.e. it is of the second order. The inset in Fig. 5 demonstrates the dependence $m^{1/\beta}(T, H_i = 0)$ at $\beta = 0.25$. The corresponding points were determined as the intersections of the ordinate axis by the dotted straight lines in Fig. 4. They correspond to $m_s^{1/\beta}(T)$, where m_s is the spontaneous magnetization. The dependence is linear at $T < T_c$ and intersects the temperature axis at $T = T_c^*$, which confirms the hypothesis that the transition into the FM phase is of the second order.

6. Conclusions

It has been found that the magnetization of the studied $La_{0.7}Sr_{0.3}MnO_3$ crystal is anhysteretic in the temperature range 295 K $< T <$ T_c^* = 353 K. The specimen did not reveal any manifestation of a magnetocrystalline anisotropy. At temperatures slightly above the magnetic ordering temperature, a non-linear feature, typical of the Griffiths phase, was found in the temperature dependence $\chi^{-1}(T, H \to 0)$. A conclusion has been drawn that this feature is a manifestation of the magnetic polaron formation in the temperature range that precedes the magnetic ordering temperature in the specimen.

The characteristic features of BA plots have been analyzed in the case where the latter are applied to systems with the Griffiths phase. Similar features were found in the BA plots drawn using the experimental data of $La_{0.7}Sr_{0.3}MnO_3$ measurements in the critical temperature range.

By analyzing the modified BA plots, a conclusion has been made that the magnetic properties of the $La_{0.7}Sr_{0.3}MnO_3$ crystal are described by different collections of critical indices in the FM (at $T < T_c$) and paramagnetic ($T > T_c$) phases. This fact was assumed to be a manifestation of the variation of the averaged exchange interaction over the specimen, rather than a consequence of the inhomogeneity of the paramagnetic phase due to magnetic polaron inclusions. Such a phenomenon can stem from a change of the charge carrier mobility at the transition from the para- into the ferrophase and the corresponding change of the charge carrier contribution to the total interaction magnitude.

1. C. Zener, Phys. Rev. **2**, 403 (1951).
2. J. Mira, J. Rivas, F.Rivadulla, C. Vazquez-Vazquez, and M.A. Lopez-Quintela, Phys. Rev. B **60**, 2998 (1999).
3. F. Rivadulla, J. Rivas, and J.B. Goodenough, Phys. Rev. B **70**, 172410 (2004).
4. S.K. Banerjee, Phys. Rev. Lett. **12**, 16 (1964).
5. S.V. Vonsovski, *Magnetism* (Wiley, New York, 1974), Vol. 2, Chap. 25.
6. K.P. Belov and L.N. Goryaga, Fiz. Met. Metalloved. **2**, 411 (1956); K.P. Belov, *Magnetic Transformations* (Fizmatgiz, Moscow, 1959) (in Russian).
7. A. Arrott, Phys. Rev. **108**, 1394 (1957).
8. R.B. Griffiths, Phys. Rev. Lett. **23**, 17 (1969).
9. A.J. Bray, Phys. Rev. Lett. **59**, 586 (1987).
10. M.A. Krivoglaz, Usp. Fiz. Nauk **111**, 617 (1973).
11. E.L. Nagaev, Phys. Rep. **346**, 763 (2001).
12. M.B. Salamon and S.H. Chun, Phys. Rev. B **68**, 014411 (2003).
13. P.Y. Chan, N. Goldenfeld, and M. Salamon, cond-mat/0603533.
14. A. Arrott and J.E. Noakes, Phys. Rev. Lett. **19**, 786 (1967).
15. K. Ghosh, C.J. Lobb, R.L. Greene S.G. Karabashev, D.A. Shulyatev, A.A. Arsenov, and Y. Mukovskii, Phys. Rev. Lett. **81**, 4740 (1998).
16. A.G. Gurevich and G.A. Melkov, *Magnetization Oscillations and Waves* (CRC Press, Boca Raton, 1996).

Translated from Ukrainian by O.I. Voitenko

КРИТИЧНА ПОВЕДІНКА КРИСТАЛА $La_{0,7}Sr_{0,3}MnO_3$ ПОБЛИЗУ ПЕРЕХОДУ У ФЕРОМАГНІТНИЙ СТАН

В.М. Калита, А.Ф. Лозенко, С.М. Рябченко, П.О. Троценко, О.І. Товстолиткін, А.М. Погорілий

Р е з ю м е

Досліджено магнітостатичні характеристики монокристала $La_{0,7}Sr_{0,3}MnO_3$ у критичному діапазоні температур. Виявлено нелінійність температурної залежності зворотної сприйнятливості у мінімальному вимірювальному полі, при температурах вищих, але близьких до температури магнітного упорядкування, характерну для фази Гріффітса. Зроблено висновок, що для досліджуваного кристала вона відбиває формування магнітних поляронів за цих температур. Проаналізовано застосування побудов Бєлова–Арротта до систем з фазою Гріффітса і виявлено їхні характерні особливості. Показано, що ці особливості присутні в побудовах Бєлова–Арротта, для експериментальних даних $La_{0,7}Sr_{0,3}MnO_3$. Отримано, що критичні властивості кристала у феромагнітній, при $T<T_c$, і в парамагнітній фазах, при $T > T_c$, описуються дещо різними наборами критичних індексів.